Collective electronic oscillator/semiempirical calculations of static nonlinear polarizabilities in conjugated molecules

S. Tretiak,[a] A. Saxena, R. L. Martin, and A. R. Bishop
Theoretical Division and Center for Nonlinear Studies, Los Alamos National Laboratory, Los Alamos, New Mexico 87545

(Received 8 September 2000; accepted 13 April 2001)

The collective electronic oscillator (CEO) approach based on the time-dependent Hartree–Fock approximation is combined with INDO/S, MNDO, AM1, and PM3 semiempirical Hamiltonians. This technique is applied to compute and analyze the static nonlinear polarizabilities of a series of donor/acceptor substituted oligomers. To mimic the experimental conditions, polarizabilities in substituted molecules are calculated for the isolated complex and in a dielectric medium, wherein the solvent contributions are incorporated using the self-consistent reaction field approach. The dielectric environment significantly increases second and third order static polarizabilities and considerably improves the agreement with experimental data. We find that calculated spectroscopic observables agree well with experimental values. We conclude that the CEO/semiempirical approach is an inexpensive and numerically efficient method of computing nonlinear molecular properties. © *2001 American Institute of Physics.* [DOI: 10.1063/1.1377035]

I. INTRODUCTION

Technologies based on organic materials for optoelectronic devices today have become a reality and in the near future may well compete with semiconductor and liquid crystal based traditional approaches. Potential technological applications include electroluminescent,[1–3] photovoltaic,[4] and optoelectronic[5–7] devices, photodetectors,[8,9] transistors,[10,11] and solid state lasers.[12–14] One of the key points in the development of such technologies is the synthesis of molecular structures with desired functionalities.

Conjugated polymers are of particular interest since delocalized π electrons along the chain are extremely polarizable in the presence of an external electric field. This leads to a large nonlinear response where the relation between static polarizability and oligomer length may be described by the scaling law $\sim n^b$, n being the number of repeat units. For short molecules the scaling exponents b_α and b_γ, associated with linear optical and third order nonlinear optical response, respectively, vary considerably ($1<b_\alpha<2$ and $2<b_\gamma<8$) depending on the polymer structure and model.[15–21] For long chains the exponents b_α and b_γ saturate to the value 1, indicating that the polarizabilities become extensive properties. Donor/acceptor substitution at chain ends enhances polarizabilities even further and even-order nonlinear responses (vanishing in unsubstituted molecules) become significant. Their scaling exponents are large for short chains ($2<b_\beta<6$).[22–25] However, contrary to the odd-order responses, even-order polarizabilities saturate and become size independent in the limit of large chains, i.e., β (rather than β/n) $\rightarrow$const and $b_\beta=0$.[20,21] Significant experimental and theoretical effort has been devoted to establish these scaling laws and many other structure/property relations.

However, accurate computations of molecular nonlinear response which reproduce experiment are still very tedious. The coupled-perturbed Hartree–Fock approach computes polarizabilities by evaluating energy derivatives of a molecular Hamiltonian perturbed by an external field.[26] Usually combined with semiempirical or *ab initio* Hamiltonians, this method involves substantial computational effort especially in the latter case. A second method uses time-dependent perturbation theory, which relates optical response to the properties of the excited states. The configuration-interaction/sum-over-states[15,27] approach involves the calculations of both the ground state and excited state wave functions and the transition dipole moments between them. This method is not necessarily size consistent (intrinsic interference effects resulting in near cancellation of very large contributions further limit its accuracy) and special care needs to be taken when choosing the right configurations. On the other hand, the experimental measurements are usually conducted in condensed phase, and therefore all spectroscopic observables are heavily influenced by intermolecular coupling in solid state or solute-solvent interactions in solution.

The recently developed collective electronic oscillator (CEO) approach[28,29] based on the time-dependent Hartree–Fock (TDHF) approximation[30,31] for many-electron wave functions is inherently size consistent. Combined with the intermediate neglect of differential overlap/spectroscopy (INDO/S)[32–34] Hamiltonian, this approach makes it possible to explore the variation of molecular polarizabilities over a broad molecular size range, all the way to the bulk. In a previous study[35] we found that the CEO coupled with other semiempirical parameterizations [e.g., the Austin model 1 (AM1),[36] parametric model 3 (PM3),[37] modified neglect of diatomic overlap (MNDO),[38] and modified intermediate neglect of differential overlap 3 (MINDO/3)[39]], which were fitted to give accurate ground state properties, also reproduce

[a]Author to whom correspondence should be addressed. Electronic mail: serg@cnls.lanl.gov

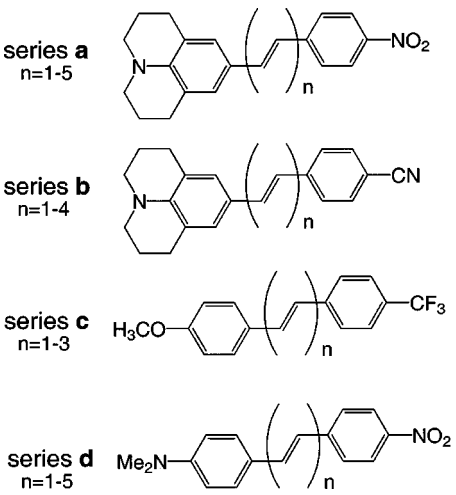

FIG. 1. Structures of push–pull donor/acceptor substituted diphenyl–polyene oligomers studied in Ref. 40.

vertical excitation energies and oscillator strengths compared to the experimental data and to INDO/S results.

In this paper we investigate how the above-described parameterizations work for nonlinear polarizabilities of extended conjugated molecules by combining the semiempirical Hamiltonians (INDO/S, AM1, PM3, MNDO, and MINDO/3) with the CEO approach.[28,29] We apply this technique to compute the first, the second, and the third order static polarizabilities (α, β, and γ), vertical excitation energies, and transition dipole moments of a series of donor/acceptor substituted oligomers. These molecules have interesting optical properties which make them particularly promising materials for device applications. Donor/acceptor compounds were synthesized and spectroscopically studied in Ref. 40. Even though the experimental measurements were corrected using the Lorentz local field factor, this correction does not yield nonlinear polarizabilities of the free molecule but rather the solute polarizabilities, which contain a contribution induced by the static reaction field (see Ref. 41 for a detailed discussion). In order to compare directly with experiment we have therefore used the self consistent reaction field (SCRF) approach, based on the Onsager model, which takes into account dielectric medium effects on the molecular excited states.

Section II briefly describes the computational method. In Sec. III we analyze the spectroscopic properties of various donor/acceptor substituted oligomers computed with different semiempirical techniques. Finally, we discuss the trends that emerge and summarize our results in Sec. IV.

II. COMPUTATIONAL METHOD

The series of donor/acceptor substituted molecules we studied (series a, b, c, and d) are shown in Fig. 1. Using GAUSSIAN 98 program,[42] each structure was optimized at the AM1 semiempirical level,[36] which provides reasonable ground-state geometries. INDO/S, AM1, PM3, MNDO, and MINDO/3 semiempirical Hamiltonians were then generated for each optimal molecular structure using ZINDO (INDO/S)[43] and MOPAC-93 (AM1, PM3, MNDO, and MINDO/3)[44] codes.[45–47]

In order to include the effects of the surrounding medium we have used the SCRF approach,[45–48] in which the interaction energy between a solute and the surrounding medium is added to the HF energy of an isolated molecule, and the total energy of the system is then minimized self consistently. In the electrically neutral solute, only the dipolar interactions contribute to the solvation energy. Assuming that the solute is separated from the solvent by a sphere of radius a_0 the expression for this Onsager dipolar term has been derived in Refs. 46 and 47. The Fock operator F^0_{mn} [49] is then modified by adding the response of a dielectric medium, resulting in

$$F_{mn}=F^0_{mn}-\frac{\epsilon-1}{2\epsilon+1}\frac{\boldsymbol{\mu}_g\cdot\boldsymbol{\mu}_{mn}}{a_0^3}, \tag{2.1}$$

where F^0_{mn} is the isolated complex Fock operator, indices n and m run over basis set functions, ϵ is the dielectric constant, and a_0 is a cavity radius. $\boldsymbol{\mu}_g$ is the ground-state dipole moment given by the expectation value of the molecular dipole operator

$$\boldsymbol{\mu}=\sum_{mn}\mu_{mn}c_m^{\dagger}c_n, \tag{2.2}$$

where $c_n^{\dagger}$ and c_n are the creation and annihilation fermions operators, respectively, of an electron in the nth atomic orbital (AO). The cavity radii a_0 were calculated with the GAUSSIAN 98 package[42] again at the AM1 level using the $Volume=Tight$ keyword, which provides a reasonable estimate for the radius of the Onsager solvent reaction field model. The approach computes the molecular volume inside a density contour of 0.001 electrons/bohr^3 using Monte Carlo integration and associates that with an effective sphere radius.[42] Although the shape of the cavity has some effect on the molecular polarizabilities,[50] the methods taking into account ''real'' molecular shapes are computationally expensive and are most appropriately utilized with accurate *ab initio* or density functional theory approaches.[50] Here, an effective sphere model captures the essential solvent effect and is a reasonable approach within semiempirical approximations. For example, this CEO/SCRF approach has been successfully applied to compute electronic excitations in biological light-harvesting complexes which are significantly affected by protein environment effects.[48]

The excited states were determined with the numerical CEO approach using each set of semiempirical Hamiltonian parameters, Onsager dipolar terms, and HF ground state density matrices. This method, described in detail elsewhere[28,29] solves equations of motion for the reduced single-electron density matrix[51,52] given by

$$\rho_{mn(t)}=\langle\Psi(t)|c_m^{\dagger}c_n|\Psi(t)\rangle, \tag{2.3}$$

where $\Psi(t)$ is the many-electron wave function. In practice, computation in the dielectric medium is conducted by replac-

ing the isolated complex Fock operator F^0_{mn} by a Fock operator in the dielectric medium F_{mn} according to the procedure outlined in Refs. 28 and 29.

When the molecule is driven by an external field, its density matrix acquires a time-dependent part. In the frequency domain, we decompose the density matrix into a ground state contribution $\overline{\rho}$ and a field-induced part

$$\rho_{mn}(\omega)=\overline{\rho}_{mn}+\delta\rho^{(1)}_{mn}(\omega)+\delta\rho^{(2)}_{mn}(\omega)+\delta\rho^{(3)}_{mn}(\omega)+\cdots, \tag{2.4}$$

where $\delta\rho^{(k)}_{mn}(\omega)$ is the kth order contribution from the incoming optical field. The diagonal elements $\delta\rho^{(k)}_{mm}$ represent the charge densities induced at the mth AO by the external field, whereas the off-diagonal elements $\delta\rho^{(k)}_{mn}$ with $m\neq n$ reflect the optically induced coherence between the mth and nth AO, which represents the probability of finding an electron–hole pair with the electron (hole) located at the mth (nth) AO. The density matrix thus provides a real-space picture of the optical response order by order in the driving field, as explored in detail in Refs. 28 and 53. The polarization can be expressed in terms of the density matrix as

$$P^{(k)}=\sum_{nm}\ \mu_{nm}\delta\rho^{k}_{mn}\,. \tag{2.5}$$

The polarizabilities α, β, and γ are related to $P^{(1)}$, $P^{(2)}$, and $P^{(3)}$, respectively.

The CEO calculates $\delta\rho^{(k)}_{mn}(\omega)$ by expanding it into a superposition of transition density matrices (denoted the *electronic normal modes*, ξ_ν), representing the electronic transition between the ground state $|g\rangle$ and an electronically excited state $|\nu\rangle$, given by

$$(\xi_\nu)_{mn}=\langle\nu|c^+_m c_n|g\rangle. \tag{2.6}$$

The electronic modes are computed as eigenmodes of the linearized TDHF equations of motion for the density matrix. [The TDHF coincides with the random phase approximation (RPA) for the linear optical response of many-electron systems (e.g., Chap. 8.5 in Ref. 30). The electronic modes are identical to the transition densities of the RPA eigenvalue equation.] The eigenfrequencies Ω_ν of these equations provide the optical transition energies.[28,29] The numerical effort involved is greatly reduced by using the oblique Lanczos algorithm.[54] These computations take into account the full orbital space (i.e., all the occupied and virtual orbitals) automatically.

In this paper we will concentrate on the off-resonant polarizabilities in the static ($\omega\rightarrow 0$) limit. With this condition the linear polarizability, for example, is given by

$$\alpha(0)=\sum_{\nu}\ \frac{2\mu^2_\nu}{\Omega_\nu}, \tag{2.7}$$

where $\mu_\nu=\mathrm{Tr}(\mu\xi_\nu)$ is the transition dipole moment for νth electronic state. In an analogous way, the second (β) and the third (γ) order off-resonant nonlinear polarizabilities can be expressed in terms of frequencies and transition dipole moments.[28,29,31]

To obtain static polarizabilities we have computed all the lowest excited states (~200–300) in the ultraviolet (UV)-visible frequency region (0–10 eV) for each molecule. These states contain most of the nonvanishing contributions to the linear and nonlinear optical responses of conjugated oligomers. In addition, the contributions to polarizabilities from the high frequency region have been taken into account using the density spectral moments algorithm,[28,29] which provides an accurate overall contribution to polarizability from the broad spectral region by computing several dominating effective states. We note that this approximation is similar to the Stieltjes imaging procedure which approximates a continuous distribution given its low-order moments.[55–57] In practice, this contribution from the high frequency region is very small, constituting only a few percent of the total polarizability magnitude.

III. DONOR/ACCEPTOR SUBSTITUTED MOLECULES

Figure 1 shows four series (a, b, c, and d) of donor/acceptor substituted molecules synthesized in a search of materials with large optical nonlinearities.[40] Reference 40 contains a detailed investigation of the spectroscopic observables of these compounds, i.e., the lowest absorbing excited state (band gap) energies and their transition dipoles, and the second and the third order static polarizabilities, using electro-optical absorption (EOA) measurements. We have calculated these properties using various semiempirical approaches coupled with the CEO method.[28,29] In our computations, these substituted molecules have been treated: (1) as isolated complexes (gas phase) with the dielectric constant $\epsilon=1$, and (2) in a dielectric medium with $\epsilon=2.219$ for the dioxane solvent used in experiment, and cavity radius a_0 computed for each compound as given in the last column of Table I. The linear absorption spectra of these compounds are dominated by a strong peak in the UV-visible region (band gap). The frequency of this transition usually redshifts with increasing strength of donor/acceptor groups and an elongating conjugated bridge. A detailed analysis of the physical phenomena emerging upon substitution using the CEO approach was conducted in Refs. 20, 21, and 28. In this paper we will concentrate on the quantitative comparison of different semiempirical approaches for molecular properties.

A. Vertical band-gap excitation energies (λ_{01})

Table I shows calculated vertical band-gap excitation energies in the dielectric medium and in the gas phase, together with their experimental values. As expected, the dielectric medium shifts excited state frequencies to the red by 0.1–0.2 eV (solvent stabilization of excited states). This redshift is smaller in the less polar molecules from the c series. To compare calculations with experiment we display the corresponding relative deviation for each compound in panel A of Fig. 2 and the average deviation for each molecular series in Table VI. It is striking to notice that computations using the Onsager solvent model significantly improve the agreement with experiment. Agreement better than 0.1 eV is observed in most computations with all semiempirical models. Such close agreement with experiment is surprising and not always to be expected. Note however, the distinct behavior of the c series where computations *consistently* underestimate the experimental energies by 0.4–0.6 eV.

TABLE I. Vertical excitation energies λ_{01} (eV) of donor/acceptor substituted oligomers shown in Fig. 1 (a, b, c, and d denote different series of substituted oligomers). CEO computations coupled with INDO/S, AM1, PM3, MNDO and MINDO/3 parameterizations were carried out in gas phase (gp) with $\epsilon = 1.0$ and in a dielectric medium (dm) with $\epsilon = 2.219$ (dioxane). The second column shows experimental data derived from electrooptic absorption (EOA) measurements in dioxane (Ref. 40). The last column displays the cavity radii a_0 used in the dielectric medium computations.

Compound No.	Expt. (dm)	INDO/S (gp)	INDO/S (dm)	AM1 (gp)	AM1 (dm)	PM3 (gp)	PM3 (dm)	MNDO (gp)	MNDO (dm)	MINDO/3 (gp)	MINDO/3 (dm)	a_0
a[1]	2.75	3.13	2.87	2.93	2.80	2.93	2.81	2.80	2.72	2.88	2.81	5.33
a[2]	2.67	2.97	2.73	2.81	2.67	2.81	2.68	2.70	2.61	2.77	2.69	5.45
a[3]	2.59	2.85	2.61	2.77	2.64	2.79	2.66	2.66	2.58	2.72	2.65	5.65
a[4]	2.57	2.76	2.51	2.72	2.59	2.74	2.62	2.62	2.53	2.66	2.59	5.78
a[5]	2.49	2.68	2.43	2.69	2.56	2.70	2.59	2.58	2.50	2.60	2.54	5.99
b[1]	3.05	3.29	3.12	2.97	2.91	2.95	2.87	2.84	2.80	2.89	2.87	5.31
b[2]	2.92	3.11	3.00	2.89	2.82	2.86	2.81	2.76	2.73	2.82	2.80	5.47
b[3]	2.80	2.94	2.81	2.80	2.73	2.80	2.72	2.69	2.65	2.73	2.71	5.60
b[4]	2.71	2.82	2.71	2.74	2.68	2.75	2.69	2.64	2.60	2.67	2.65	5.90
c[1]	3.81	3.54	3.47	3.24	3.20	3.30	3.27	3.00	2.96	3.16	3.11	4.93
c[2]	3.57	3.25	3.18	3.07	3.04	3.13	3.09	2.87	2.84	2.99	2.94	5.16
c[3]	3.35	3.04	2.97	2.94	2.91	2.99	2.95	2.77	2.73	2.85	2.80	5.32
d[1]	2.81	3.12	2.93	2.98	2.84	2.99	2.84	2.82	2.71	2.95	2.85	4.96
d[2]	2.72	3.01	2.77	2.87	2.70	2.89	2.72	2.73	2.60	2.83	2.72	5.06
d[3]	2.65	2.88	2.62	2.80	2.63	2.82	2.66	2.67	2.55	2.75	2.64	5.27
d[4]	2.61	2.77	2.52	2.74	2.60	2.77	2.63	2.62	2.52	2.68	2.58	5.54
d[5]	2.52	2.69	2.43	2.69	2.56	2.72	2.59	2.58	2.49	2.61	2.53	5.76

B. Transition dipole moments (μ_{01})

Table II displays computed transition dipoles of the lowest (band gap) state. The dielectric medium has a very small effect on the dipole magnitudes. Compared to experimental data (relative deviations are shown in panel B of Fig. 2 and Table VI) computations usually overestimate experiment by 10%–20%. We also notice that AM1, PM3, and MNDO dipoles are generally smaller than that of INDO/S and compare more favorably with experiment. Trends vary significantly from one series to another.

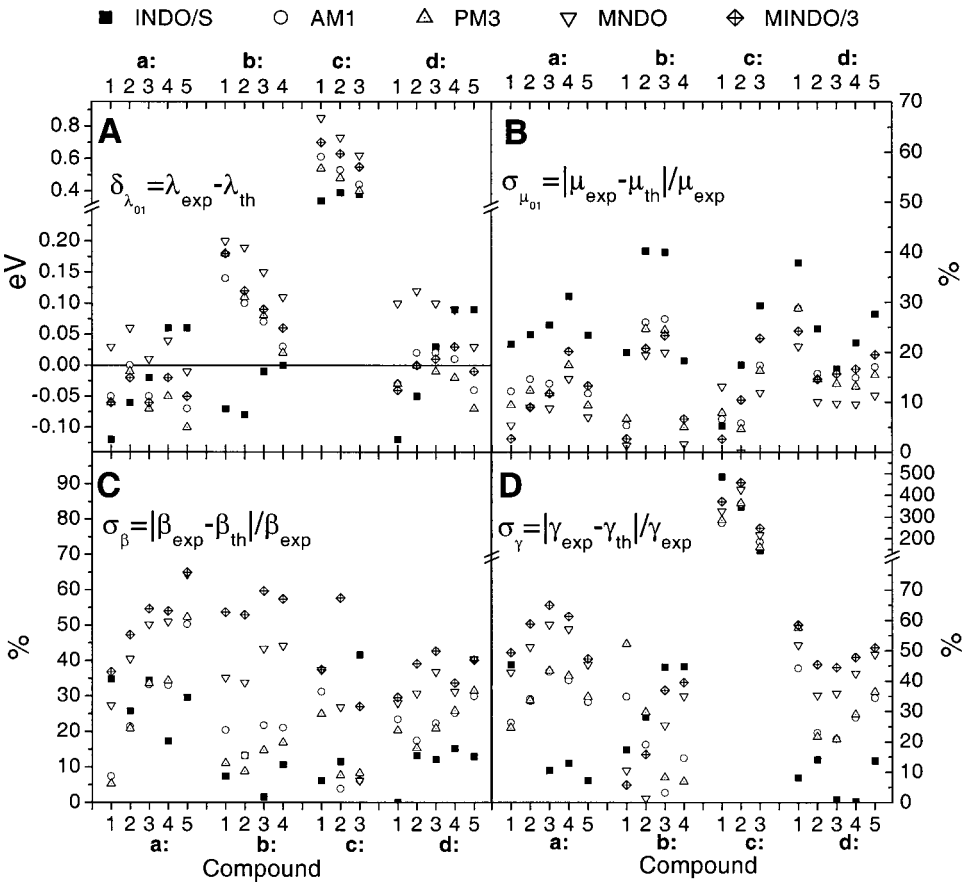

FIG. 2. Deviations of magnitudes of spectroscopic observables computed in the dielectric medium using model Hamiltonians from the corresponding experimental values for molecular series a, b, c, and d.

TABLE II. Transition dipole moments μ_{01} (D). Same as Table I.

Compound No.	Expt.	INDO/S (gp)	INDO/S (dm)	AM1 (gp)	AM1 (dm)	PM3 (gp)	PM3 (dm)	MNDO (gp)	MNDO (dm)	MINDO/3 (gp)	MINDO/3 (dm)
a[1]	7.4	8.9	9.0	7.8	8.3	7.7	8.1	7.4	7.8	7.2	7.6
a[2]	8.9	11.0	11.0	9.8	10.2	9.5	10.0	9.3	9.7	9.3	9.7
a[3]	10.2	12.7	12.8	11.3	11.6	11.0	11.4	10.8	11.1	11.1	11.4
a[4]	10.9	14.1	14.3	12.7	13.1	12.5	12.8	12.2	12.5	12.8	13.1
a[5]	12.8	15.6	15.8	14.0	14.3	13.8	14.0	13.5	13.7	14.3	14.5
b[1]	7.5	8.8	9.0	7.7	7.9	7.7	8.0	7.2	7.4	7.2	7.3
b[2]	7.7	10.8	10.8	9.5	9.7	9.5	9.6	9.0	9.2	9.2	9.3
b[3]	9.0	12.6	12.6	11.2	11.4	11.0	11.2	10.6	10.8	11.0	11.1
b[4]	12.0	14.2	14.2	12.6	12.8	12.5	12.6	12.1	12.2	12.7	12.8
c[1]	7.6	8.0	8.0	6.9	7.1	6.9	7.0	6.5	6.6	7.2	7.4
c[2]	8.6	10.1	10.1	9.0	9.1	8.9	9.0	8.5	8.6	9.3	9.5
c[3]	9.2	11.9	11.9	10.7	10.8	10.7	10.7	10.2	10.3	11.2	11.3
d[1]	6.6	9.1	9.1	8.1	8.5	8.1	8.5	7.6	8.0	7.9	8.2
d[2]	8.9	10.9	11.1	9.9	10.3	9.8	10.2	9.4	9.8	9.8	10.2
d[3]	10.2	12.6	11.9	11.5	11.8	11.3	11.6	10.9	11.2	11.5	11.8
d[4]	11.4	14.1	13.9	12.9	13.1	12.7	12.9	12.3	12.5	13.0	13.3
d[5]	12.3	15.5	15.7	14.2	14.4	13.9	14.2	13.5	13.7	14.4	14.7

C. Static linear polarizabilities ($\alpha(0)$)

Static linear polarizabilities ($\alpha(0)$) are shown in Table III. Experimental data are not available for these quantities. We notice a small increase in the polarizability magnitudes in the dielectric medium caused by related redshifts of frequencies [the denominator in Eq. (2.7)]. AM1 and PM3 values are very similar. Compared with INDO/S, AM1 and PM3 polarizabilities are smaller but larger than that of MNDO. These trends follow from a decrease in the magnitude of the relevant transition dipoles [the numerator in Eq. (2.7)] when comparing INDO/S with AM1, PM3, and MNDO.

D. Static quadratic polarizabilities ($\beta(0)$)

Static quadratic polarizabilities ($\beta(0)$) are displayed in Table IV. We first notice a dramatic increase, by a factor of ~ 3, of the computed polarizability caused by the solvent. This greatly improves agreement with experiment and indicates a significant enhancement of nonlinear coupling among electronic modes [see Eqs. (5.10) in Ref. 31] due to the dielectric medium. To compare calculations with experiment, the relevant relative deviations are shown in panel C of Fig. 2 and in Table VI. Although the agreement appears less striking even after taking into account solvent effects (within

TABLE III. Static linear polarizability $\alpha(0)$ (10^{-24} esu). Same as Table I.

Compound No.	INDO/S (gp)	INDO/S (dm)	AM1 (gp)	AM1 (dm)	PM3 (gp)	PM3 (dm)	MNDO (gp)	MNDO (dm)	MINDO/3 (gp)	MINDO/3 (dm)
a[1]	57.7	58.0	55.6	58.5	56.0	58.6	54.5	56.8	50.9	52.7
a[2]	77.5	78.7	70.6	76.0	71.0	75.0	69.6	73.4	67.8	71.1
a[3]	96.3	97.9	85.6	90.9	84.3	89.5	84.5	88.4	84.8	88.2
a[4]	112.6	122.1	101.4	108.6	100.2	106.5	100.3	105.1	103.3	107.9
a[5]	135.6	146.8	119.0	126.6	116.7	123.4	116.8	122.2	123.2	128.4
b[1]	53.5	55.5	55.8	57.3	57.8	59.3	52.8	53.9	50.8	51.4
b[2]	70.7	73.6	68.3	70.1	70.5	72.4	66.5	68.0	66.7	67.5
b[3]	91.9	96.8	83.9	87.2	86.1	88.9	82.4	84.4	84.8	85.8
b[4]	113.6	119.3	100.2	103.6	101.2	104.7	98.1	100.6	103.6	104.5
c[1]	43.0	43.7	44.2	46.0	43.1	44.1	42.2	43.0	42.6	43.5
c[2]	59.6	60.9	56.3	56.7	55.1	55.8	55.4	56.5	57.6	58.0
c[3]	79.3	81.5	70.2	71.5	70.0	70.1	69.8	71.3	74.0	76.3
d[1]	51.7	55.3	51.8	55.6	53.5	55.7	52.0	55.2	48.6	51.3
d[2]	69.7	76.4	66.7	72.9	66.0	71.8	66.6	71.5	64.4	68.7
d[3]	89.7	98.6	82.6	89.5	81.4	88.4	82.1	88.0	81.9	87.6
d[4]	99.7	110.6	98.9	106.8	97.5	104.6	98.3	104.5	100.8	106.7
d[5]	133.6	147.0	116.3	124.8	114.3	122.0	115.2	121.6	120.2	126.7

TABLE IV. Static second order polarizability $\beta(0)$ (10^{-30} esu). Same as Table I. Experimental values of β in parentheses were inferred from EFISH measurements (Refs. 22 and 58).

Compound No.	Expt. (dm)	INDO/S (gp)	INDO/S (dm)	AM1 (gp)	AM1 (dm)	PM3 (gp)	PM3 (dm)	MNDO (gp)	MNDO (dm)	MINDO/3 (gp)	MINDO/3 (dm)
a[1]	95(113)	41	62	51	88	55	90	43	69	39	60
a[2]	163(156)	69	121	67	128	69	129	54	97	49	86
a[3]	247(209)	83	162	82	165	84	164	66	123	60	112
a[4]	300(297)	102	248	95	201	96	197	75	147	71	138
a[5]	480(367)	148	338	106	239	107	229	83	171	80	168
b[1]	54	32	50	30	43	33	48	24	35	19	25
b[2]	68	44	77	39	59	40	62	30	45	22	32
b[3]	129	64	131	59	101	63	110	45	73	34	52
b[4]	242	93	216	72	191	77	201	73	135	60	103
c[1]	16	11	17	5	11	6	12	7	10	7	10
c[2]	26	14	23	18	27	19	28	22	33	27	41
c[3]	48	39	68	28	45	28	44	31	51	38	61
d[1]	64 (72)	36	64	28	49	29	51	26	46	27	45
d[2]	143(130)	60	124	60	118	63	121	52	99	47	87
d[3]	206(211)	75	181	74	160	77	163	64	130	58	118
d[4]	282	85	239	86	211	88	209	73	194	68	187
d[5]	371	117	323	97	260	98	254	81	221	79	222

50% for all semiempirical models), we recall that cubic dependencies of β from a combination of transition dipoles and excited state frequencies greatly enhance any deviations of the latter from the experimental values. On the other hand, the two-level model used to infer static second order polarizabilities from results of EOA experiments itself constitutes a significant approximation and deviates from corresponding electric field induced second harmonic (EFISH) measurements[22,58] by 10%–30% (see values given in parentheses, col. 2 of Table IV). Computations underestimate β magnitudes for series a, b, and d, and overestimate polarizabilities for c molecules. AM1, PM3, and especially MNDO polarizabilities are smaller than that of INDO/S, which follows from a hierarchy of transition dipole magnitudes.

E. Static cubic polarizabilities ($\gamma(0)$)

Static cubic polarizabilities ($\gamma(0)$) are displayed in Table V and relevant absolute deviations are given in panel D of Fig. 2 and in Table VI. We observe a significant increase in γ by a factor of 2 induced by the solvent; however, this is less pronounced than β enhancement. Computational values in series a, b, and d underestimate experimental results by less than 60%, which is reasonable considering the subtle nature

TABLE V. Static third order polarizability $\gamma(0)$ (10^{-36} esu). Same as Table I. Experimental values of γ in parentheses were derived from third harmonic generation experiments (Ref. 40).

Compound No.	Expt. (dm)	INDO/S (gp)	INDO/S (dm)	AM1 (gp)	AM1 (dm)	PM3 (gp)	PM3 (dm)	MNDO (gp)	MNDO (dm)	MINDO/3 (gp)	MINDO/3 (dm)
a[1]	1160(818)	438	634	577	855	534	875	452	662	411	587
a[2]	2228(1621)	754	1481	791	1468	809	1478	671	1085	611	916
a[3]	3733(3363)	1749	3338	1122	2125	1136	2110	958	1543	874	1305
a[4]	4736(5150)	2091	4121	1495	2829	1491	2759	1273	2029	1192	1832
a[5]	8358	3521	7750	2900	5591	2880	5445	2616	4555	2580	4400
b[1]	310	253	364	332	418	365	472	289	343	261	292
b[2]	561	458	719	515	668	559	728	464	553	426	472
b[3]	1339	1281	1937	925	1296	1005	1450	796	998	757	844
b[4]	2110(1857)	2152	3055	1262	1801	1378	1962	1079	1370	1061	1275
c[1]	−7	35	41	23	26	25	27	27	30	24	33
c[2]	−22	85	98	92	101	90	102	99	116	96	123
c[3]	67	135	159	164	191	168	175	177	213	180	234
d[1]	680	384	624	230	379	240	288	212	327	191	282
d[2]	1670	756	1434	691	1286	708	1308	636	1079	565	910
d[3]	2498	1330	2522	1002	1975	1015	1977	912	1600	830	1387
d[4]	3611(3777)	1687	3602	1356	2603	1359	2565	1221	2074	1154	1883
d[5]	5149(5845)	3080	5853	1751	3378	1730	3273	1561	2636	1513	2524

TABLE VI. Average deviations of spectroscopic observables calculated in the dielectric medium (gas phase) from the corresponding experimental values. Average absolute ($\overline{\delta}=\Sigma_n^N|\eta_{\text{th}}^{(n)}-\eta_{\text{exp}}^{(n)}|/N$) and relative ($\overline{\sigma}=\Sigma_n^N|\eta_{\text{th}}^{(n)}-\eta_{\text{exp}}^{(n)}|/\eta_{\text{exp}}^{(n)}/N$) errors are computed for each series of molecules shown in Fig. 1. Signs + (−) indicate that theory systematically overestimates (underestimates) experiment.

Deviations	Series	INDO/S	AM1	PM3	MNDO	MINDO/3
$\overline{\delta}_{\lambda_{01}}$ (eV)	a	0.06 (+0.26)	+0.04 (+0.17)	+0.06 (+0.18)	0.03 (+0.06)	+0.04 (+0.11)
	b	+0.04 (+0.17)	−0.08 (0.03)	−0.09 (0.05)	−0.17 (−0.14)	−0.11 (−0.09)
	c	−0.37 (−0.3)	−0.53 (−0.5)	−0.47 (−0.44)	−0.73 (−0.7)	−0.63 (−0.58)
	d	0.08 (+0.23)	0.02 (+0.15)	+0.03 (+0.18)	−0.09 (+0.02)	0.02 (+0.1)
$\overline{\sigma}_{\mu_{01}}$ (%)	a	+24 (+25)	+14 (+10)	+12 (+8)	+9 (+6)	+11 (+10)
	b	+29 (+30)	+16 (+14)	+15 (+13)	+11 (+8)	+13 (+13)
	c	+17 (+17)	10 (10)	10 (10)	8 (9)	10 (12)
	d	+27 (+26)	+18 (+15)	+17 (+14)	+12 (+9)	+18 (+15)
$\overline{\sigma}_{\beta}$ (%)	a	−28 (−63)	−29 (−63)	−29 (−62)	−47 (−71)	−51 (−73)
	b	8 (−47)	−19 (−53)	−13 (−50)	−39 (−62)	−56 (−70)
	c	20 (−32)	14 (−47)	14 (−44)	24 (−37)	41 (−27)
	d	−11 (−61)	−24 (−64)	−23 (−63)	−34 (−69)	−37 (−70)
$\overline{\sigma}_{\gamma}$ (%)	a	−23 (−59)	−35 (−64)	−36 (−64)	−36 (−69)	−56 (−72)
	b	+34 (−10)	18 (−18)	24 (19)	−18 (−28)	−25 (−33)
	c	+332 (+260)	+272 (+230)	+270 (+240)	+325 (+267)	+360 (+250)
	d	7.4 (−48)	−30 (−63)	−33 (−62)	−43 (−66)	−49 (−69)

of third order polarizability. It is proportional to the fourth power of the combination of transition dipoles and excited state frequencies. In addition, the two level model (TLM) used to derive the experimental γ is oversimplified (compare TLM results to more accurate data derived from third harmonic generation experiments[40] which are given in parentheses, col. 2 of Table V). In these series, the INDO/S approach is the most accurate, and demonstrates excellent agreement with experiment, within 30%. AM1, PM3, and especially MNDO values are smaller than that of INDO/S which again follows from the hierarchy of transition dipole magnitudes. We notice a significant discrepancy between theory and experiment for the c series. Very small third order polarizabilities compared to the other molecules have been observed in experiment. Here, even though the computed polarizabilities are smaller compared to other series, they are too large compared to experiment. In addition, experimental negative signs in c[1] and c[2] molecules are not reproduced. We will discuss this discrepancy in Sec. IV

IV. DISCUSSION

We have computed the lowest absorbing excited state (band gap) energies and their transition dipoles, and the first, the second, and the third order static polarizabilities of several series of donor/acceptor substituted diphenyl–polyene oligomers with various sizes. These molecules are fairly small compared to limiting chain lengths when polarizabilities are expected to saturate.[19–21] Therefore, nonlinear polarizabilities of the considered substituted oligomers grow rapidly with increasing molecular size.

Our computational approach combines different semiempirical Hamiltonians (INDO/S,[32] AM1,[36] PM3,[37] MNDO,[38] MINDO/3)[39] with the CEO[28,29] technique which utilizes the TDHF approximation for the many-electron wave function.[30,31] To include dielectric environment effects we used the SCRF approach based on the Onsager dipolar model.

Computational results were compared with the experimental data reported in Ref. 40. Figure 3 shows the total deviation of computed values from the experimental results averaged over a, b, and d compounds. The computed excitation energies are reasonably accurate using any semiempirical model, and systematically improved when taking into account the solvent environment. Transition dipoles calculated with semiempirical Hamiltonians parameterized for the ground state (AM1, PM3, and MNDO) compare slightly more favorably with experiment than INDO/S values. The dielectric medium has very little effect on the transition dipole moments. Thus the simplest Onsager spherical cavity model, where an effective sphere radius is associated with the ''real'' molecular volume, performs fairly well in addressing the dielectric medium effects for the linear absorption spectrum. We must note that the small error observed in these calculations for the band gap is not always to be expected, and errors in this property will propagate into the hyperpolarizabilities.

The solvent environment has a dramatic effect on the magnitudes of nonlinear polarizabilities and has to be taken into account to reproduce experimental results. Polarizabilities computed with the INDO/S Hamiltonian parametrized for spectroscopic purposes shows the best comparison with experimental results (on average 16% and 20% accuracy for the second and the third order static polarizabilities, respectively). In addition, the comparison with the experiment for nonlinear polarizabilities of such large molecular systems is complicated because significant approximations (two- and three-level models or projection of the frequency dependent polarizability to the static limit) are usually invoked to estimate experimental values.[40] For example, the two-level approximation for the second-order polarizability typically

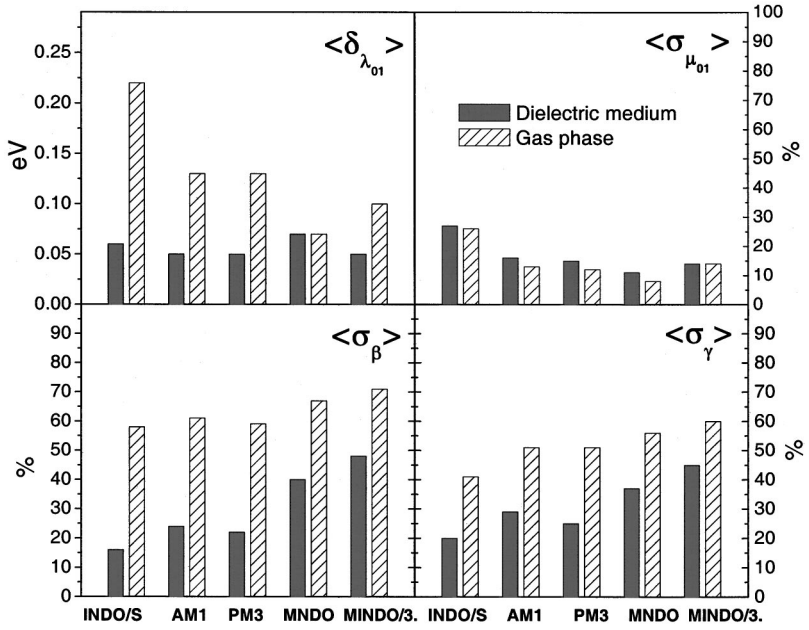

FIG. 3. Total averaged deviations of magnitudes of computed spectroscopic observables for a, b, and d series in the dielectric medium and in the gas phase using model Hamiltonians, from the corresponding experimental values.

overestimates its value,[26] whereas in the three-level approximation for the third-order response, the position, and the properties of the third state are usually not available from experiment.[40] Nevertheless, the agreement with experiment for the series a, b, and d is encouraging. An additional caveat concerns the use of a more sophisticated solvent model to describe the dielectric medium effects. One possibility is that an elliptical cavity approximation would be more appropriate for such elongated donor/acceptor molecules. Although this approach is a straightforward generalization of the spherical cavity model,[59] the parameters of the ellipsoid are not well defined for conjugated systems such as considered in the present paper. Most likely they will be related to the effective conjugation lengths rather than to physical molecular dimensions. Therefore, the elliptical model calculations are still rarely applied to electronic structure calculations of large molecules[60] compared to the spherical model.[45–48] In order to get a feel for how our computed properties would be modified, we have conducted several test calculations with prolate ellipsoid cavity for molecules in series a. We kept the cavity volume constant while increasing ellipticity. These computations show that in general solvation effects are decreased and our results move toward the gas-phase results as the ellipticity is increased. In series a, for reasonable ranges of the ellipsoid parameters this yields values about midway between our gas phase and spherical cavity approximation results. Even in this ellipsoidal limit, there is a significant signature of solvation. Future theoretical studies are clearly required to build a more accurate description of solvation effects on excitation energies in these large molecular systems.[61]

We have not included the spectroscopic observables computed for c oligomers in the above analysis. They require a separate discussion. We notice that experimental nonlinear polarizabilities of these compounds are much smaller compared to the other molecules because the donor and acceptor groups are weak. Their excitation energies are therefore comparable to that of the unsubstituted oligomers, e.g., the band-gap excitation energy of c[1] compound (3.81 eV) is only weakly redshifted compared to the band gap of stilbene (3.98 eV).[62] This suggests a large torsional disorder in c molecules, whereas a, b, and d compounds have strong donor and acceptor substitutions, which in turn straighten the molecular backbone to maximize donor/acceptor charge transfer. AM1 geometry optimization results in nearly planar structures for all molecules. The ground state energy curve along the torsion motion coordinates is very shallow in the c series and much steeper in a, b, and d molecules. However, this torsional disorder has a very strong effect on the π-electron delocalization along the conjugated backbone, and therefore tends to significantly vary the excitation energies and polarizabilities. For example, a 40° torsion of c[1] leads to a blueshift of the INDO/S calculated energy by 0.3 eV (which corresponds to the experimental value), and decreases the third order polarizability from 41×10^{-36} esu (0° torsion) to 11×10^{-36} esu (40° torsion). The latter compares well with experiment. In addition, for the c series two and three level approximations for $\beta(0)$ and $\gamma(0)$ are less accurate than that for the other molecules since the intramolecular charge transfer is very weak, and thus the experimental values derived from EOA measurements have to be taken with caution.[63] These arguments suggest a need for more advanced computational approaches[62] or experimental studies to obtain optimal structures of c molecules. These may be used as an input for the CEO computations for further reliable comparison with experiment.

We conclude that a reasonably accurate computation of excitation energies, transition dipoles, and nonlinear static polarizabilities is possible by combining INDO/S, AM1, PM3, or MNDO semiempirical parameterizations with the CEO technique for excited states. Careful choice of the optimal geometry and inclusion of dielectric medium effects significantly improve the quantitative comparison with the experimental data. The latter ingredient is extremely impor-

tant for computing nonlinear polarizabilities which may be drastically enhanced by the solvent environment.

ACKNOWLEDGMENTS

This work was performed under the auspices of the U.S. Department of Energy and the LDRD program at LANL. S.T. gratefully acknowledges the support of a LANL Director's Postdoctoral Fellowship. The numerical computations were performed using the resources of the Center for Nonlinear Studies at Los Alamos National Laboratory.

[1] J. Burroughes, D. D. C. Bradley, A. Brown, R. Marks, K. Mackay, R. Friend, P. Burns, and A. Holmes, Nature (London) **347**, 539 (1990).
[2] D. Braun and A. J. Heeger, Appl. Phys. Lett. **58**, 1982 (1991).
[3] Q. B. Pei, G. Yu, C. Zhang, Y. Yang, and A. J. Heeger, Science **269**, 1086 (1995).
[4] G. Yu, J. Gao, J. C. Hummelen, F. Wudl, and A. J. Heeger, Science **270**, 1789 (1995).
[5] H. Sirringhaus, N. Tessler, and R. H. Friend, Science **280**, 1741 (1998).
[6] P. K. H. Ho, D. S. Thomas, R. H. Friend, and N. Tessler, Science **285**, 233 (1999).
[7] A. Dodabalapur, Z. Bao, A. Makhja, J. C. Laquindanum, V. R. Raju, Y. Feng, H. E. Katz, and J. Rogers, Appl. Phys. Lett. **73**, 142 (1998).
[8] G. Yu, K. Pakbaz, and A. J. Heeger, Appl. Phys. Lett. **64**, 3422 (1994).
[9] H. Yu, B. R. Hsieh, M. A. Abkowitz, S. A. Jenekhe, and M. Stolka, Synth. Met. **62**, 265 (1994).
[10] H. E. Katz, J. Mater. Chem. **7**, 369 (1997).
[11] D. J. Gundlach, Y. Y. Lin, T. N. Jackson, and D. G. Schlom, Appl. Phys. Lett. **71**, 3853 (1997).
[12] F. Hide, M. A. Diaz Garcia, B. J. Schwartz, M. R. Andersson, Q. B. Pei, and A. J. Heeger, Science **273**, 1833 (1996).
[13] N. Tessler, G. J. Denton, and R. H. Friend, Nature (London) **382**, 695 (1996).
[14] S. V. Frolov, M. Shkunov, Z. V. Vardeny, and K. Yoshino, Phys. Rev. B **56**, R4363 (1997).
[15] J. L. Brédas, C. Adant, P. Tackyx, A. Persoons, and B. M. Pierce, Chem. Rev. **94**, 243 (1994).
[16] J. F. Heflin, K. Y. Wong, Q. Zamani-Khamini, and A. F. Garito, Phys. Rev. B **38**, 1573 (1988).
[17] D. C. Rodenberger and A. F. Garito, Nature (London) **359**, 309 (1992).
[18] G. P. Agrawal, C. Cojan, and C. Flytzanis, Phys. Rev. B **17**, 776 (1978).
[19] S. Tretiak, V. Chernyak, and S. Mukamel, Phys. Rev. Lett. **77**, 4656 (1996).
[20] S. Tretiak, V. Chernyak, and S. Mukamel, Chem. Phys. Lett. **287**, 75 (1998).
[21] S. Tretiak, V. Chernyak, and S. Mukamel, Chem. Phys. **245**, 145 (1999).
[22] M. Blanchard-Desce, C. Runser, A. Fort, M. Barzoukas, J.-M. Lehn, V. Bloy, and V. Alain, Chem. Phys. **199**, 253 (1995).
[23] M. Blanchard-Desce, R. Woltmann, S. Lebus, J.-M. Lehn, and P. Kramer, Chem. Phys. Lett. **243**, 526 (1995).
[24] M. Blanchard-Desce, J.-M. Lehn, M. Barzoukas, C. Runser, A. Fort, G. Puccetti, I. Ledoux, and J. Zyss, Nonlinear Opt. **10**, 23 (1995).
[25] M. Blanchard-Desce, J.-M. Lehn, M. Barzoukas, I. Ledoux, and J. Zyss, Chem. Phys. **181**, 281 (1994).
[26] D. R. Kanis, M. A. Ratner, and T. J. Marks, Chem. Rev. **94**, 195 (1994).
[27] J. L. Brédas, J. Cornil, D. Beljonne, D. A. Dos Santos, and Z. Shuai, Acc. Chem. Res. **32**, 267 (1999).
[28] S. Tretiak, V. Chernyak, and S. Mukamel, J. Am. Chem. Soc. **119**, 11408 (1997).
[29] S. Tretiak, V. Chernyak, and S. Mukamel, J. Chem. Phys. **105**, 8914 (1996).
[30] P. Ring and P. Schuck, *The Nuclear Many-Body Problem* (Springer, New York, 1980).
[31] V. Chernyak and S. Mukamel, J. Chem. Phys. **104**, 444 (1996).
[32] J. A. Pople and G. A. Segal, J. Chem. Phys. **43**, S136 (1965); J. A. Pople, D. L. Beveridge, and P. Dobosh, *ibid.* **47**, 2026 (1967).
[33] J. Ridley and M. C. Zerner, Theor. Chim. Acta **32**, 111 (1973).
[34] M. C. Zerner, G. H. Loew, R. F. Kirchner, and U. T. Mueller-Westerhoff, J. Am. Chem. Soc. **102**, 589 (1980).
[35] S. Tretiak, A. Saxena, R. L. Martin, and A. R. Bishop, Chem. Phys. Lett. **331**, 561 (2000).
[36] M. J. S. Dewar, E. G. Zoebisch, E. F. Healy, and J. J. P. Stewart, J. Am. Chem. Soc. **107**, 3902 (1985).
[37] J. J. P. Stewart, J. Comput. Chem. **10**, 210 (1989).
[38] M. J. S. Dewar and W. Thiel, J. Am. Chem. Soc. **99**, 4899 (1977).
[39] M. J. S. Dewar, R. C. Bingham, and D. H. Lo, J. Am. Chem. Soc. **97**, 1285 (1975).
[40] V. Alain, S. Rédoglia, M. Blanchard-Desce, S. Lebus, K. Lukaszuk, R. Wortmann, U. Gubler, C. Bosshard, and P. Günter, Chem. Phys. **245**, 51 (1999).
[41] R. Wortmann and D. M. Bishop, J. Chem. Phys. **108**, 1001 (1998).
[42] M. J. Frisch, G. W. Trucks, H. B. Schlegel *et al.*, GAUSSIAN 98, Revision A.7, Gaussian, Inc., Pittsburgh PA, 1998.
[43] M. C. Zerner, ''ZINDO, A General Semiempirical Program Package,'' Department of Biochemistry, University of Florida: Gainesville, FL, 1998.
[44] J. J. P. Stewart, MOPAC *Manual* (Schrödinger Inc. and Fujitsu Limited, Portland, OR, 2000).
[45] M. G. Cory, M. C. Zerner, X. Hu, and X. K. Schulten, J. Phys. Chem. **102**, 7640 (1998).
[46] G. Karlsson and M. C. Zerner, Int. J. Quantum Chem. **7**, 35 (1973).
[47] G. Karlsson and M. C. Zerner, J. Phys. Chem. **96**, 6949 (1992).
[48] S. Tretiak, C. Middleton, V. Chernyak, and S. Mukamel, J. Phys. Chem. **104**, 9540 (2000).
[49] A. Szabo and N. S. Ostlund, *Modern Quantum Chemistry: Introduction to Advanced Electronic Structure Theory* (McGraw-Hill, New York, 1989).
[50] R. Cammi, B. Mennucci, and J. Tomasi, J. Phys. Chem. A **102**, 870 (1998).
[51] E. R. Davidson, *Reduced Density Matrices in Quantum Chemistry* (Academic, New York, 1976).
[52] R. McWeeny and B. T. Sutcliffe, *Methods of Molecular Quantum Mechanics* (Academic, New York, 1976).
[53] S. Mukamel, S. Tretiak, T. Wagersreiter, and V. Chernyak, Science **277**, 781 (1997).
[54] V. Chernyak, S. Tretiak, M. Schulz, E. V. Tsiper, and S. Mukamel, J. Chem. Phys. **113**, 36 (2000).
[55] P. W. Langhoff, C. T. Corcoran, J. S. Sims, F. Weinhold, and R. M. Glover, Phys. Rev. A **14**, 1042 (1976).
[56] R. L. Martin, W. R. Daasch, and E. R. Davidson, J. Chem. Phys. **71**, 2375 (1979).
[57] R. L. Martin and J. S. Cohen, Phys. Lett. **110A**, 95 (1985).
[58] M. Blanchard-Desce, V. Alain, L. Midrier, R. Wortmann, S. Lebus, C. Glania, P. Kramer, A. Fort, J. Muller, and M. Barzoukas, J. Photochem. Photobiol. A **105**, 115 (1997).
[59] C. J. F. Bottcher, *Theory of Electric Polarization* (Elsevier, Amsterdam, 1973).
[60] M. M. Kerelson, T. Tamm, A. R. Karitzky, S. J. Cato, and M. C. Zerner, Tetrahedron Comput. Methodol. **2**, 295 (1989).
[61] G. J. Tawa, R. L. Martin, and L. R. Pratt, Int. J. Quantum Chem. **64**, 143 (1997). Y
[62] V. Molina, M. Merchán, and B. O. Roos, J. Phys. Chem. A **101**, 3478 (1997).
[63] M. Blanchard-Desce (private communications).